ACCEPTED MANUSCRIPT

Computer-aided approach for the identification of lead molecules as the inhibitors of cholinesterase's and monoamine oxidases: Novel target for the treatment of Alzheimer's disease

SYEDA ABIDA EJAZ[1]*, MUBASHIR AZIZ[1], AMMARA FAYYAZ[1], TANVEER A. WANI[2], AND SEEMA ZARGAR[3]

[1]*Department of Pharmaceutical Chemistry, Faculty of Pharmacy, The Islamia University of Bahawalpur, Bahawalpur 63100, Pakistan,* [2]*Department of Pharmaceutical Chemistry, College of Pharmacy, King Saud Univeristy, P.O.Box 2457, Riyadh 11451, Saudi Arabia, and* [3]*Department of Biochemistry, College of Science, King Saud Univeristy, P.O. Box 22452, Riyadh 11451, Saudi Arabia*

Abstract: Molecular docking is a promising and reliable technology for the purpose of discovering lead compounds via virtual screening. In addition to allowing for the testing of a large number of compounds, it also allows for the determination of how the selected compounds inhibit the targeted protein/receptor based on the scoring function and ranking. Because selective cholinesterase and monoamine oxidase inhibitors play a critical role in the treatment of Alzheimer's disease, this research focuses on elucidating the mechanism of binding interactions of a few quinolone derivatives within the active sites of cholinesterase (acetyl-cholinesterase (AChE) and butyrylcholinesterase (BChE) and monoamine oxidase (MAO) (monoamine oxidase A &B). As a result of these discoveries, it is possible that the newly identified inhibitors will be used as lead compounds in the development of novel enzyme inhibitors for the treatment of specific diseases, hence enabling the development of novel therapeutic approaches.

Keywords: molecular docking; acetyl-cholinesterase (AChE); butyrylcholineesterase (BChE); active pocket; monoamine oxidases A & B, Alzheimer disease.

INTRODUCTION

The actions of brain neurons, particularly neurotransmission, are grouped into systems of individually distinct neurons, neurotransmitters, neuromodulators, receptors, and hormones. The monoaminergic and cholinergic systems are essential in these systems. A crucial component of the cholinergic system of neurotransmission is the neurotransmitter acetylcholine.[1] Neuromuscular

---

synapses, the brain, and autonomic ganglia all contain acetylcholine (ACh) which is fast acting. Two enzymes; acetylcholinesterase (AChE; EC 3.1.1.7) and butyrylcholinesterase are present in tissues that catalyze the breakdown of acetylcholine (BChE; EC 3.1.1.8).[2] The two enzymes are both glycoproteins that can either be membrane-bound or soluble. AChE is a critical enzyme in cholinergic neurotransmission on both the central and peripheral level. It is mostly membrane-bound and located in the neuromuscular junctions and synapses between neurons in the central nervous system, where it inhibits the activity of acetylcholine (Ach) produced during nerve stimulation.[3] The enzyme is also present in soluble forms and linked with the erythrocyte membrane. BChE is found in a broad variety of human tissue types. It is expressed in several different groups of neurons in the human brain that are not connected with AChE, as well as glial cells. BChE is significantly more abundant in the serum than AChE is. BChE, like AChE, is a soluble enzyme that may also be membrane-bound.[4] AChE is highly effective at hydrolyzing Ach, but its catalytic site is buried deep inside a deep cavity, which restricts its ability to cleave esters with heavier acyl groups.[5] As compared to AChE, butyrylcholinesterase has a bigger cavity and is a less selective esterase capable of cleaving a variety of esters with larger acyl groups.[6]

The network of monoamine neurotransmission systems, each of which is regulated by a unique monoamine neurotransmitter, is known as the monoamine neurotransmission system. These include the dopaminergic, noradrenergic, and serotonergic systems, which are each regulated by the neurotransmitters dopamine, noradrenaline, and serotonin, respectively.[7] Two isoforms of the monoamine oxidase (MAO) enzyme, MAO A and MAO B, are involved in the oxidative deamination of biogenic amines, including neuroamines, vasoactive amines, and exogenous amines and hence regulates the concentration of amine neurotransmitters and numerous amine medications.[8] Due to their location on the mitochondrial outer membrane, the MAO flavoproteins metabolize amines inside the cell. Each MAO has a different tissue concentration, with the two versions functioning identically in the human liver. MAO B is highly expressed in platelets, glial cells, and serotonergic neurons, whereas MAO A is expressed primarily in the stomach, placenta, and dopaminergic and noradrenergic neurons.[9] Despite having the identical catalytic center structure, with substrate-orienting tyrosinase leading to covalently bound FAD,[10] the two forms exhibit distinct intrinsic activity (kcat and Km values) with each substrate. Serotonin is metabolized mostly by MAO A in the human brain, but dopamine is metabolized by both forms.11

Alzheimer's disease (AD) is the most common neurodegenerative ailment, affecting millions of individuals worldwide, including 5% of the over-65 population. The primary clinical manifestation of AD is increasing memory loss and other abnormalities in brain function, such as aberrant behavior and impairments in language, comprehension, and visual-spatial abilities.[12]
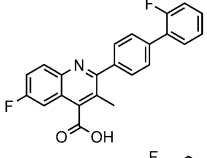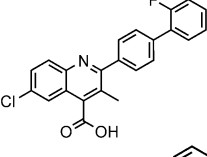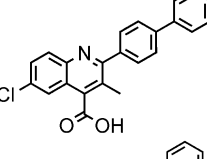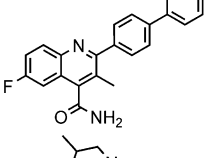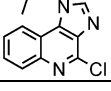
It has been postulated that BChE collaborates with AChE in the brain to regulate ACh neurotransmission when ACh levels become excessive, especially given that AChE is inhibited by high concentrations of its substrate.[13] In the average human brain, BChE activity is lower than AChE activity, whereas AD patients have much higher BChE/AChE ratios,[14] indicating that BChE inhibition can get critical as AD advances. This has generated the concept that inhibiting both ChEs may result in enhanced therapeutic advantages or that inhibiting BChE alone may be advantageous.[15]

The first therapy methods for AD were aimed at boosting cholinergic transmission in the brain, in accordance with the "cholinergic hypothesis" of memory loss. Among the several strategies used to raise synaptic ACh levels, inhibiting acetylcholinesterase (AChE) has shown to be the most effective. Inhibiting the enzyme butyrylcholinesterase (BuChE), which is present in trace amounts in normal brains but is elevated in the brains of AD patients with plaques and tangles, may enhance cholinergic transmission.[16] Dopamine, serotonin, and noradrenaline, which are all metabolized by MAO or catechol-O-methyltransferase (COMT), are reduced as a consequence of other neurons being gradually eliminated in AD. MAO inhibitors have long been used as antidepressants, and an early study against Parkinson's disease led in the acceptance of l-deprenyl (Selegiline) as a disease-delaying medication for the condition. Thus, MAO inhibitors may promote amine neurotransmission and have beneficial biochemical effects in the therapy of Alzheimer's disease.[17] Increased MAO B levels have been found in AD patients' brains as a result of increased astrogliosis,[18] suggesting that combined MAO A/B inhibition may be an effective AD treatment. MAO inhibitors' beneficial features also include a decrease in the generation of reactive oxygen species, which may contribute to greater neuronal damage.[19]

Current novel therapeutic approaches suggest that drugs targeting a single target may be insufficient for treating multifactorial neurodegenerative diseases such as Alzheimer's disease (AD), Parkinson's disease (PD), Huntington's disease (HD), and amyotrophic lateral sclerosis (ALS), which are all characterized by the coexistence of multiple etiologies. These include, but are not limited to, the development of oxidative stress (OS) and reactive oxygen species (ROS), protein misfolding and aggregation, mitochondrial dysfunction, inflammation, metal dyshomeostasis, and accumulation at neurodegenerative sites.[20] Thus, it is plausible to assume that AD treatment will likely need a combination of drugs to address the disease's many clinical manifestations. Due to the multifactorial character of AD and the variety of brain pathways involved in its control,[21] multi-targeted ligands have been widely investigated as potential therapeutic candidates with favorable benefits in AD treatment.[22]

The current study is focused on the identification of quinolone derivatives as the inhibitors of either class of enzymes i.e., cholinesterases (AChE and BChE) and monamine oxidases (MAO-A and MAO-B). Quinolones have been previously identified for their anti-bacterial activity in the treatment of various infections. They are specifically designed to selectively target two bacterial topoisomerase enzymes: DNA gyrase that targets Gram-negative bacteria and topoisomerase IV that effects Gram-positive bacteria.[23] The approved Quinolone derivative drug Tacrine lowers AChE levels in Alzhiemer's disease. One study showed that Quinolone derivatives were active against AChE with an IC_{50} values ranging from 7.31 to 88.10 μM.[24] The long-term use, however, of quinolones is not recommended as it may be carcinogenic to adults and arthropathogenic in children. However, they can be used for the short-term treatment and symptomatic management of Alzheimer's disease. This study will lead a comprehensive knowledge of the structures, activity correlations, and roles of the discovered inhibitors/drug-like compounds which promises well enough for the future development of novel pharmaceuticals. The following compounds were selected for this study.

Table 1: List of the chosen derivatives

Code	IUPAC Name	Structure
3	6-fluoro-2-[4-(2-fluorophenyl) phenyl]-3-methylquinoline-4-carboxylic acid	
3-A	6-chloro-2-[4-(2-fluorophenyl) phenyl]-3-methylquinoline-4-carboxylic acid	
3-B	6-chloro-3-methyl-2-(4-phenylphenyl) quinoline-4-carboxylic acid	
3-C	6-fluoro-3-methyl-2-(4-phenylphenyl) quinoline-4-carboxamide	
4	4-chloro-1-(2-methylpropyl) imidazole[4,5-c] quinoline	

1-(2-methylpropyl) chromeno[3,4-d] triazol-4-one
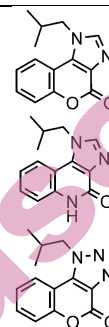
EXPERIMENTAL

Molecular Docking:

In the present work, we employed molecular docking using MOE Software[23] to predict the inhibitory mechanism of chosen quinolone and quinoline derivatives. The crystal structure of the chosen target (AChE, PDB id: 4BDT), (BChE, PDB id: 4BDS), (MAO-A, PDB id: 2Z5Y), and (MAO-B, PDB id: 2V5Z) was obtained from the protein data bank and utilized for further research. The force field MMFF94x with an RMSD gradient of >0.01 kcal/mol/Å was used to minimize the energy of the selected quinoline and quinolone compounds. Additionally, when the ligands and protein were created, charges were assigned and hydrogen atoms were added to all molecules, the MOE site finder tool was used to locate the binding site, as mentioned before. For considering the conformational flexibility parameters, we have employed a simulation approach for docking purposes in which the ligand is allowed to interact with the groove of a targeted protein after a series of moves in its conformational space. These moves include changes in the structures of ligands either internally by rotating the torsional angles or the number of rotatable bonds, or externally by translation and rotation. Each rotation of ligand produced intermolecular interactions with the targeted protein. This approach is preferred for taking into account the conformational flexibility of ligands, and it may take longer time depending upon the performance of computing system. In a current study, two series of ligands were docked. Quinoline derivatives have four rotatable bonds, whereas quinolone derivatives have only two rotatable bonds. By employing a simulation approach, ligands were allowed to interact with targeted protein through torsional angles. The rigid receptor model was employed and total numbers of poses were set to 100. Finally, the MOE software was used to produce 3D and 2D poses for further investigation.[25] The docking of all the compounds was reconfirmed by SeeSAR Analysis.[26]

RESULTS AND DISCUSSION

AChE Results*:*

As shown in table 1, the derivative **4** which has the most binding score -26.9 kJ/mol showed binding interactions. The amino acid His447 formed carbon hydrogen bonding with the hydrogen attached with nitrogen in the imidazole. Similarly, Trp86 and Tyr337 formed π-π stacked interaction with imidazole and pyridine ring. The Binding Energy and bonding and non-bonding interactions of quinolone derivatives within the active pocket of AChE is given in Supplementary file.

The Alkyl interaction was formed with the amino acid Pro446 which formed interaction with the chlorine attached with the pyridine ring and similarly, the amino acid Trp439 formed π-alkyl interaction with the chlorine attached with the pyridine ring. The amino acids which formed Van der Waals interactions were Ile451, Glu202, Ser203, Tyr133, Gly122, Gly121, Asp74, Tyr341, Thr83, Tyr77. The derivative **4-C** which has the best binding score -26.5 kJ/mol after the derivative 5 formed the following interactions. The amino acids Trp86, Tyr337 which formed π-π stacked interaction with the imidazole ring and with pyridine ring. The derivative **4-A** which has the binding score -26.1 kJ/mol. The amino acids Glu202 and Gly126 which formed carbon hydrogen bond with the oxygen attached with pyran ring and with the hydrogen of imidazole ring. The π -sigma interaction was formed with the amino acid Trp86. Similarly, the binding score of the derivative **4-B** is -25.6 kJ/mol made C-H bond with the amino acid Thr83 involving oxygen attached with pyran ring. The π-π stacked interaction involved with the amino acids Trp86, Tyr337 with the imidazole and pyridine ring. The derivative **3-C** showed binding score -22.3 kJ/mol and formed interactions. The amino acid Trp86 formed conventional hydrogen bonding with the amino group and the amino acid Gly126, Gly121 formed carbon hydrogen bonding with the oxygen attached with pyridine ring and the derivative **3** that has the binding score -21.8 kJ/mol formed alkyl interaction with amino acid His447 with the substitution on pyridine ring. The amino acid Trp86 formed π-sigma bond with the substituted benzene ring. Similarly, the derivative **3-A** has the binding score -20.8 kJ/mol formed conventional hydrogen bonding with the amino acid His447. The amino acids Tyr119, Tyr133, Leu130 formed π-alkyl interaction with chlorine attached with the benzene ring and the derivative **3-B** which has a binding score of -20.7 kJ/mol formed conventional hydrogen bonding involving amino acid His447 with the hydrogen attached with the oxygen in pyridine ring. The amino acids Tyr119, Tyr133 and Leu130 which formed alkyl and π-alkyl chlorine attached with the benzene ring.

AChE 3D
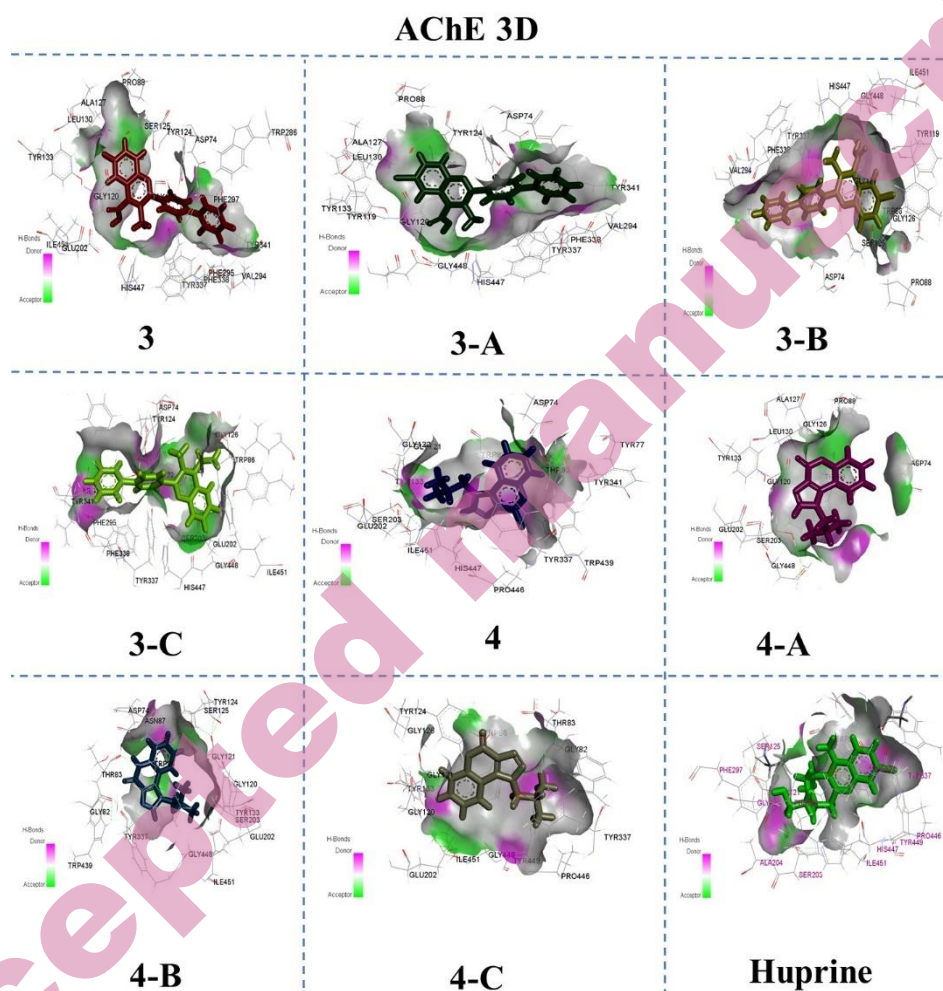
Figure 1. 3D binding interactions of selected compounds within the active pocket of AChE

SeeSAR Analysis

The best derivative 4 was subjected to SeeSAR analysis in order to predict the virtual visualization of binding interactions. Green colored coronas were used to indicate the structural components of potent compounds, whereas red colored coronas were used to indicate those parts that had an adverse impact on binding interactions. A colorless corona was used to shade structural elements that made little contribution. Corona size predicts the contribution of a structural component. SeeSAR visualization of potent derivative **4** is given in (Figure 2). Hyde energy of favorable corona (green colored) for **4** was -8.3 kJ/mol while the hyde energy of unfavorable corona (red colored) was 9.0 kJ/mol.
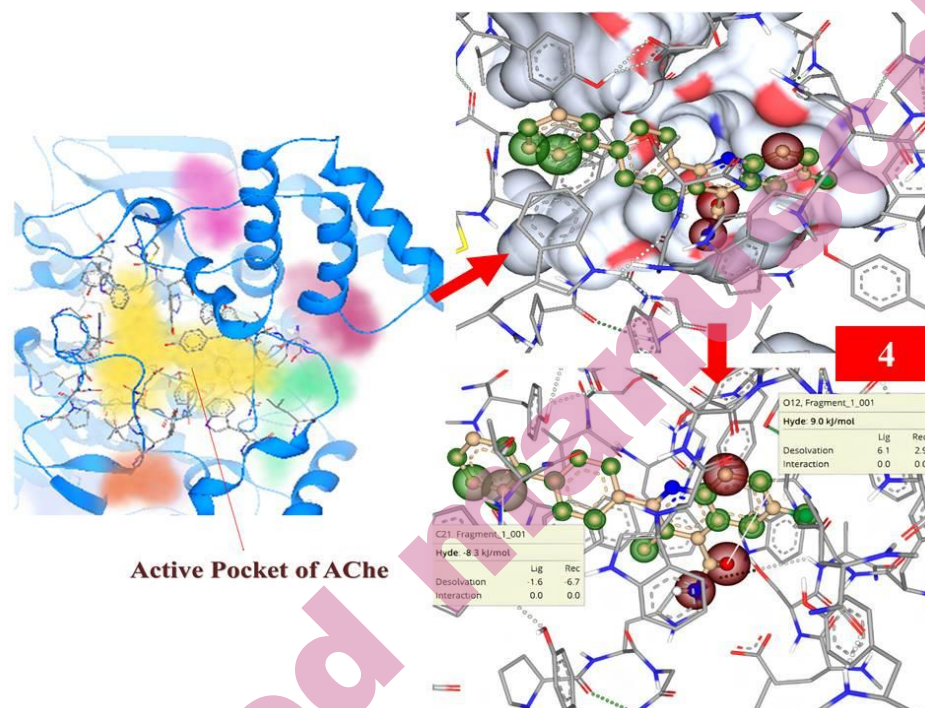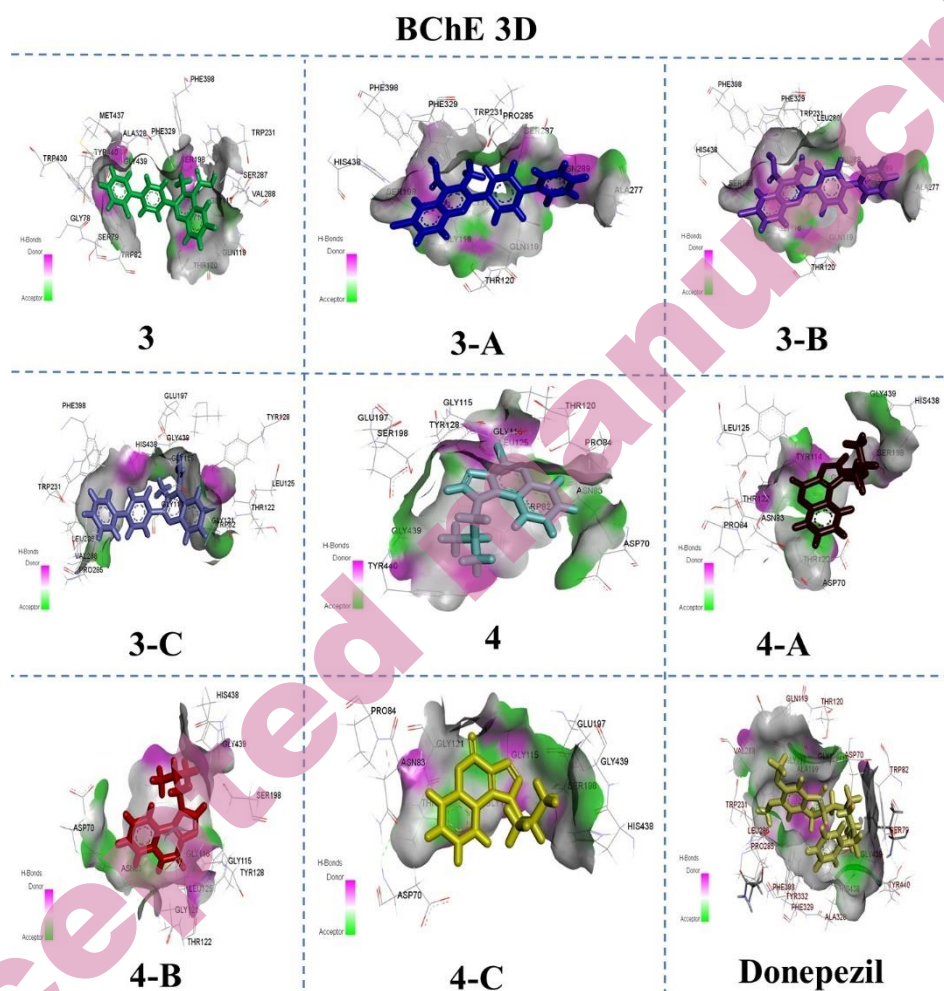
Figure 2. Left; SeeSAR analysis of the active pocket of AChE. Right; showing docked conformations with coronas. Red colored coronas represent undesirable characteristics, green colored coronas show favorable contributions, and colorless coronas represent no structural component contribution.

BChE results

As shown in table 3, the derivative **3-C** which has the most binding score -29.3648 kJ/mol showed binding interactions. The amino acids Thr122, Tyr128 and Gly121 which formed conventional hydrogen bonding and carbon hydrogen bonding with the chlorine attached with the benzene ring. Similarly, the amino acids Phe329 and Trp231 made π-π T shaped interaction with the benzene ring. Binding Energy and bonding and non-bonding interactions of quinolone derivatives within the active pocket of BChE is provided in Supplementary file.

The π-Alkyl interaction was formed with the amino acid His438 and Leu286 which formed interaction with the substitution attached with the pyridine ring and with the benzene ring. Similarly, the amino acid Trp82 formed π-sigma interaction with the substituted benzene ring. The amino acid Glu197 formed unfavorable acceptor-acceptor with the oxygen attached with pyridine ring. The amino acids which formed Van der Waals interactions were Val288, Pro285, Gly116, Leu125, Gly115, Ile442, Gly439, Phe398. The derivative **3** which has the best binding score -28.6 kJ/mol after the derivative 1 produced the following interactions. The amino

acids Gly116 which formed π-π T shaped interaction with the pyridine ring and with substituted benzene ring. The amide-π stacked interaction was formed with the amino acid Trp82 involving the benzene ring and the amino acid Ala328 formed π-alkyl interaction with the substituted benzene ring. The derivative **3-B** which has the binding score -26.6 kJ/mol. The amino acids Gly117 and Ser198 which formed conventional hydrogen bond with the oxygen attached with pyridine ring. The amide-π stacked interaction was formed with the amino acid Gly116. Similarly, the binding score of the derivative **3-A** is -26.5 kJ/mol formed conventional hydrogen bond with the amino acid Gly117 and Ser198 involving oxygen attached with pyridine ring. The amide-π stacked interaction involved with the amino acids Gly116 with the pyridine ring and substituted benzene ring. The amino acid His438 formed π-alkyl interaction with the chlorine. The derivative **4-B** showed binding score -25.3 kJ/mol and formed interactions. The amino acid Tyr128 formed conventional hydrogen bonding with the oxygen attached with the pyridine ring and the amino acid His438 formed -alkyl interaction with the dimethylpropane and the derivative **7** which has the binding score -25.2 kJ/mol formed hydrogen bond and C-H bond with the amino acid Trp82, Tyr128 and Gly121 with the oxygen attached with the pyridine ring. Similarly, the derivative **8** has the binding score -24.9328 kJ/mol formed hydrogen bond with the amino acid Gly121 with the oxygen attached with pyridine ring. The amino acids His438 formed π-alkyl interaction with dimethylpropane and the derivative **5** which has a binding score of -24.1 kJ/mol formed π-alkyl interaction involving amino acid Tyr128 with chlorine attached with pyridine ring. The amino acid Trp82 formed π-sigma interaction with pyridine ring.

BChE 3D

Figure 3. 3D binding interactions of selected compounds within the active pocket of BChE

SeeSAR Analysis

SeeSAR analysis of the best derivative **3-C** was executed which anticipate virtual display of binding interactions. Green colored coronas were used to positively present the structural components of potent compounds, whereas red colored coronas were used to favorably convey the structural members that had a detrimental impact on binding interactions. A colorless corona was used to represent structural elements that made little contribution. Corona size determines the contribution of a structural component. SeeSAR visualization of potent derivative **3-C** is given in figure 4. Hyde energies of favorable coronas

(green colored) for **3-C** was -4.7 and -4.5 kJ/mol while the hyde energy of unfavorable corona (red colored) was 13.8 kJ/mol.
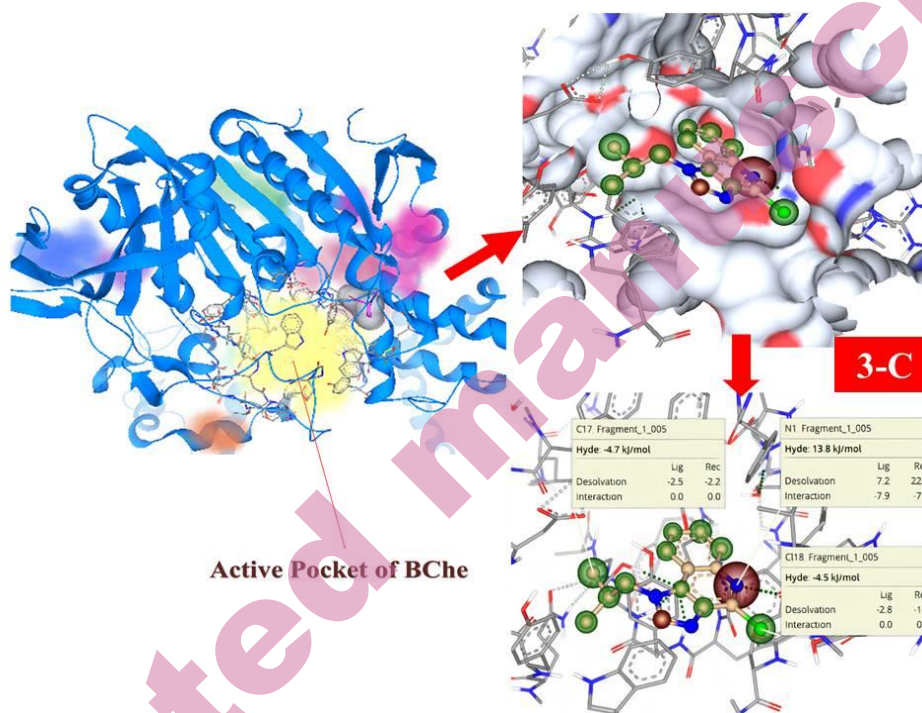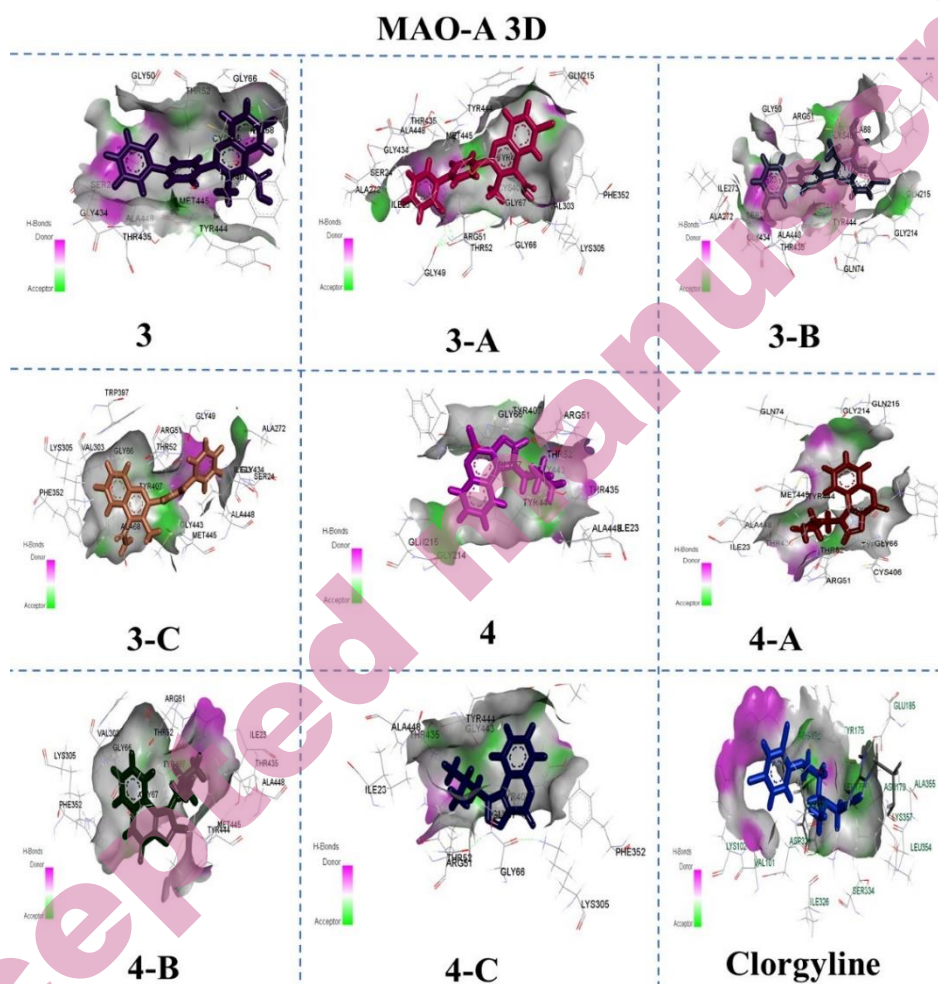

Figure 4. Left; SeeSAR analysis of the active pocket of BChE. Right; showing docked conformations with coronas. Red colored coronas show unfavorable interactions whereas green coronas are representing favorable contributions and colorless coronas are showing no contribution of components.

MAO-A Results:

As shown in table 4, the derivative **3** which has the most binding score -37.5 kJ/mol showed binding interactions. The amino acids Thr52 and Ile23 which formed conventional hydrogen bond and π-donor hydrogen bond with the fluorine attached with the benzene ring and with the benzene ring. Similarly, the amino acid Trp397 which formed π-π stacked interaction with the substituted benzene ring. Binding Energy and bonding and non-bonding interactions of quinolone derivatives within the active pocket of MAO-A is given in Supplementary file.

Amide-π stacked interaction was formed involving the amino acid residue Tyr444 with the benzene ring. The amino acids Ala448 and Met445 formed π-alkyl interaction with the substituted benzene ring and with the benzene ring. The amino acids which formed Van der Waals interactions were Ser24, Gly434, Thr435, Gly66, Lys305, Phe352, Ala68, Gly50. The derivative **3-A** which has the

best binding score -37.5 kJ/mol after the derivative 1 formed the following interactions. The substituted benzene ring and the pyridine ring produced conventional hydrogen bonds and carbon hydrogen bonds with the amino acids Arg51, Thr52, and Tyr444. The benzene ring and the amino acid Met444 established π -Sulphur interaction. The pyridine ring was involved in the formation of the amide-stacked interaction with the amino acid Tyr407. The derivative **3-B** which has the binding score -37.1 kJ/mol. The amino acids Tyr444 which formed carbon hydrogen bond with the benzene and pyridine ring. The amino acid Ala448 and Cys406, Met445 formed alkyl and π-alkyl interactions with the benzene and the pyridine ring. The π-cation interaction was formed with the amino acid Arg51. Similarly, the binding score of the derivative **3-C** is -36.9 kJ/mol formed amide-π stacked interaction involving the amino acid Trp397 with the substituted benzene ring. The amino acid Tyr407 formed π-π stacked interaction with the pyridine ring. The amino acids Met445 and Ala448 formed π-alkyl interaction with the benzene and pyridine ring. The derivative **4** showed binding score of -30.3 kJ/mol. The amino acid Tyr407 and Gly443 formed carbon hydrogen bond with the hydrogen attached with the nitrogen in imidazole ring. The amino acid Arg51 and Phe352 formed alkyl and π-alkyl interaction with the imidazole ring and with the chlorine attached with benzene ring and similarly, the derivative **4-C** which has the binding score -29.5 kJ/mol formed carbon hydrogen bond with the amino acid Tyr407 and Gly443 with the hydrogen of dimethylpropan and the amino acid Arg51 formed alkyl interaction with the imidazole ring. Similarly, the derivative **4-A** has the binding score -29.1 kJ/mol formed carbon hydrogen bond with the amino acid Tyr407 with the hydrogen of dimethylpropan. The amino acids Met445 formed π-alkyl interaction with benzene ring and the derivative **4-B** which has a binding score of -28.4 kJ/mol formed carbon hydrogen bond involving the amino acid Gly67 with the hydrogen of dimethylpropan and the amino acid Arg51 and Met445 formed alkyl and π-alkyl interaction imidazole ring.

MAO-A 3D

Figure 5. 3D binding interactions of selected compounds within the active pocket of MAO-A

SeeSAR Analysis

SeeSAR analysis of the best derivative **3** was executed which anticipate virtual display of binding interactions. Green colored coronas were used to favorably identify the structural elements of potent compounds, whereas red colored coronas were used to distinguish those elements that had a negative impact on binding interactions. Colorless coronas were used to shade structural elements that made no contribution. The size of the corona predicts the contribution of structural components. SeeSAR display of potent derivative **3** is given in Figure 6. Hyde energies of favorable coronas (green colored) for **3** was -8.7 and -4.8 kJ/mol while the hyde energy of unfavorable corona (red colored) was 12.1 kJ/mol.

EJAZ *et al.*
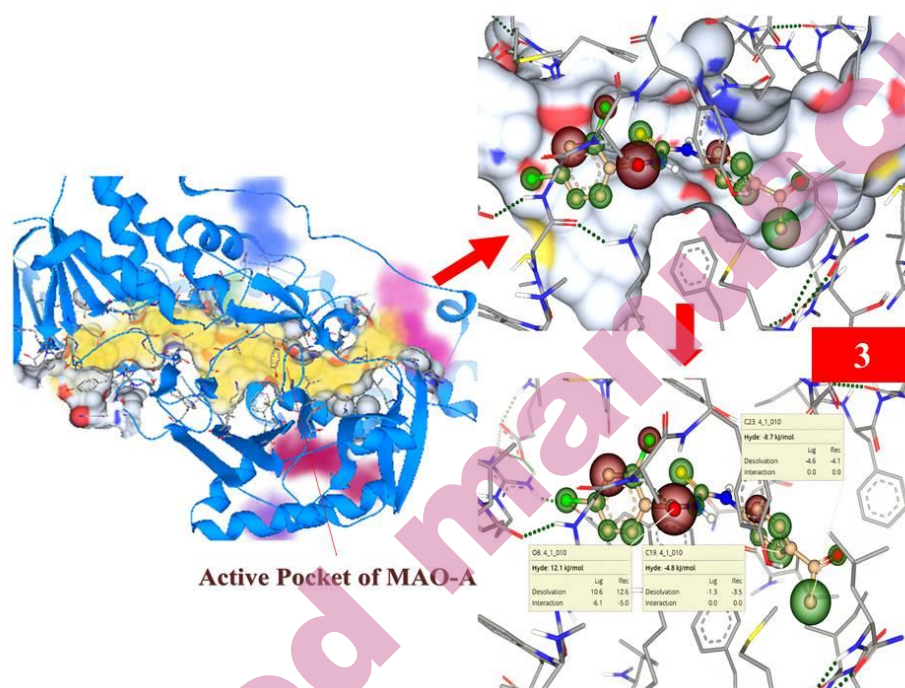
Figure 6. Left; SeeSAR analysis of the active pocket of MAO-A. Right; showing docked conformations with coronas. Colorless coronas represent no structural component contribution, while green coronas indicate favorable contributions and red coronas indicate undesirable aspects.

MAO-B Results:

The derivative **3-B** which has the most binding score -36.9 kJ/mol showed binding interactions. The amino acids Trp388 and Tyr398 established interactions with the substituted benzene ring and the pyridine, respectively, that were π-π stacked and a T shape, respectively. The amino acids Ala439 and Lys296 and Val294 and Cys397 and Phe343 developed alkyl and π-alkyl interactions with the benzene, substituted benzene ring and with chlorine attached with benzene ring. Binding Energy and bonding and non-bonding interactions of quinolone derivatives within the active pocket of MAO-B is provided in Supplementary file.

The -cation interaction was also observed involving the amino acid Arg42 with the benzene ring. The amino acids which formed Van der Waals interactions were Ala263, Ile264, Gly13, Ile14, Thr43, Gly57, Leu56, Tyr435, Gly434, Thr426, Gly425, Ser15. The derivative **3-A** which has the best binding score -36.7 kJ/mol after the derivative 1 formed the following interactions. The amino acids Gly58 and Arg42 which formed carbon hydrogen bond and conventional hydrogen bond with the oxygen attached with pyridine ring and with fluorine and benzene

ring. The amino acid Thr43 formed π-cation interaction with the fluorine attached with benzene ring. The derivative **3-C** which has the binding score -35.9 kJ/mol. The amino acid Ala439 formed alkyl interactions with the benzene ring. The π- π interaction was formed involving the amino acid Arg42 with the benzene ring. Similarly, the binding score of the derivative **3** is -34.9 kJ/mol formed amide-π stacked interaction involving the amino acid Gly57 with the substituted benzene ring. The amino acid Tyr398 formed π-π stacked interaction with the substituted benzene ring. The amino acids Met445 and Ala439 formed π-alkyl interaction with the substituted benzene ring. The π-cation interaction was formed involving the amino acid Arg42 with the benzene ring. The derivative **4-C** showed binding score -28.7 kJ/mol and formed interactions. The amino acid Tyr398 formed carbon hydrogen bond with the dimethylpropan. The amino acid Val294 and Arg42 formed alkyl and π-alkyl interaction with the dimethylpropan and with the imidazole ring. The π-Sulphur interaction was formed involving the amino acid Cys397 with the imidazole ring and similarly, the derivative **4** which has the binding score -28.6 kJ/mol formed alkyl and π-alkyl interaction involving the amino acid Val294, Tyr398 and Met436 with the substituted benzene ring and with the imidazole ring. The derivative **7** has the binding score -28.5 kJ/mol formed carbon hydrogen bond with the amino acid Tyr398 with the hydrogen of dimethylpropan. The amino acid Gly57 formed amide-π stacked interaction involving the amino acid with the imidazole ring and the derivative **4-A** which has a binding score of -27.7 kJ/mol formed conventional hydrogen bond involving the amino acid Lys296 and the amino acid which formed carbon hydrogen bond Tyr398, Arg42 with the oxygen of pyridine ring and with the hydrogen of imidazole ring.

MAO-B 3D
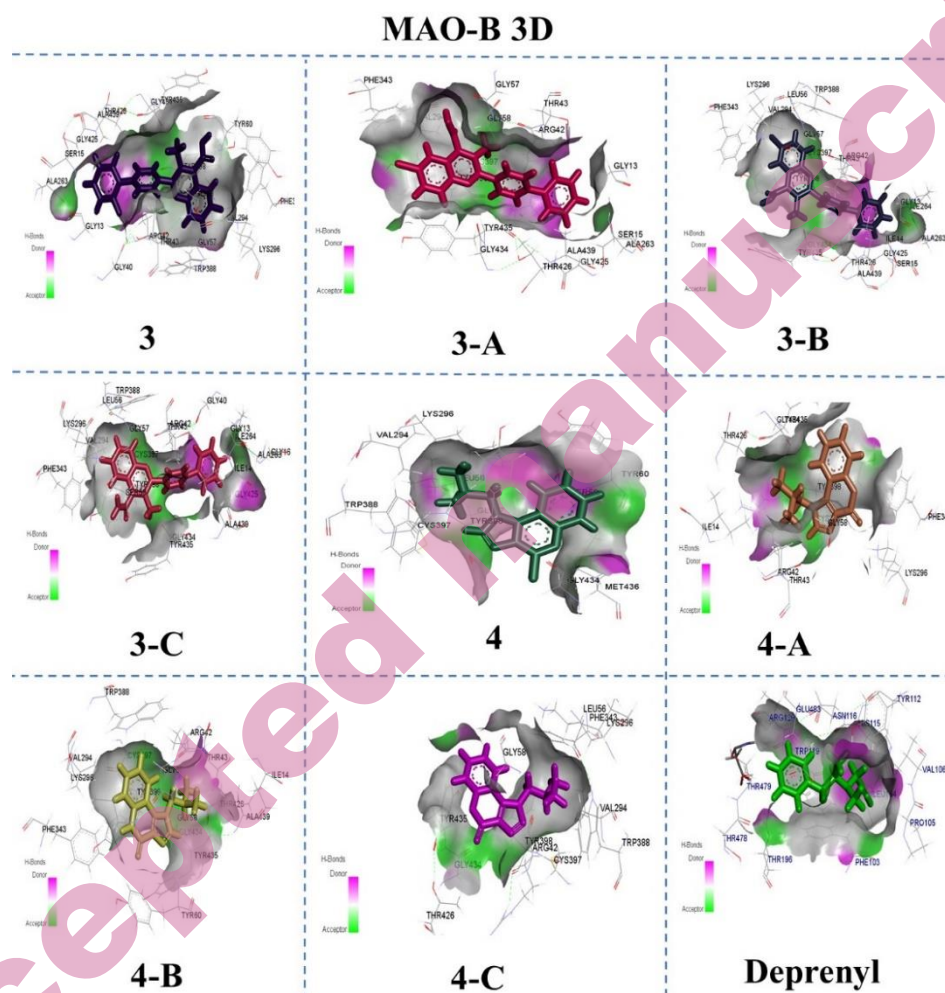
Figure 7. 3D binding interactions of selected compounds within the active pocket of MAO-B

SeeSAR Analysis

SeeSAR analysis of the best derivative **3-B** was executed which anticipate virtual display of binding interactions. Green colored coronas were used to favorably present structural elements of active compounds, whereas red colored coronas are used to present elements that had a negative effect on binding interactions. A colorless corona was used to shade structural elements that made zero contribution. Corona size reflects the contribution of a structural element. SeeSAR visualizations of potent derivative **3-B** is given in figure 8. Hyde energies of favorable coronas (green colored) for **3-B** was -5.4 and -5.3 kJ/mol.
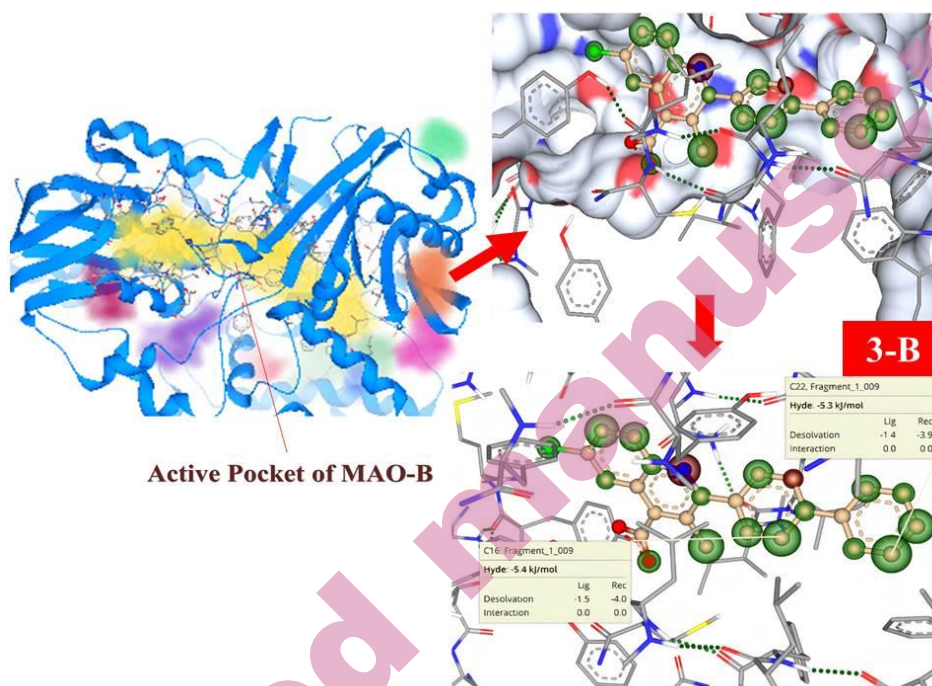
Figure 8. Left; SeeSAR analysis of the active pocket of MAO-B. Right; showing docked conformations with coronas. Red colored coronas show unfavorable features whereas green colored coronas represent favorable contributions and colorless coronas are showing no contribution of structural components.

CONCLUSION

To identify new BChE inhibitors, which may serve as a potential lead candidate for the treatment of AD, the structure-based virtual screening method was used to examine the interactions between proteins and ligands. The PubChem database was filtered, and then screened for both AChE and BChE protein. Furthermore, their predicted inhibition constant values and binding energy values were both correlated. The results revealed that these compounds might serve as a foundation for the future development of novel BChE inhibitors.

SUPPLEMENTARY MATERIAL

Additional data are available electronically at the pages of journal website: https://www.shd-pub.org.rs/index.php/JSCS/article/view/12309, or from the corresponding author on request.

Conflict of Interest: No conflicts of interest have been disclosed by the authors.

Competing interest: The authors declare no competing interests.

И З В О Д

РАЧУНАРСКИ ПОТПОМОГНУТ ПРИСТУП ЗА ИДЕНТИФИКАЦИЈУ НАВОДЕЋИХ (LEAD) МОЛЕКУЛА ЗА ИНХИБИТОРЕ ХОЛИНЕСТЕРАЗА И МОНОАМИН ОКСИДАЗА: НОВЕ МЕТЕ ЗА ТРЕТИРАЊЕ АЛЦХАЈМЕРОВЕ БОЛЕСТИ

SYEDA ABIDA EJAZ[1], MUBASHIR AZIZ[1], AMMARA FAYYAZ[1], TANVEER A. WANI[2], AND SEEMA ZARGAR[3]

[1]*Department of Pharmaceutical Chemistry, Faculty of Pharmacy, The Islamia University of Bahawalpur, Bahawalpur 63100, Pakistan,* [2]*Department of Pharmaceutical Chemistry, College of Pharmacy, King Saud Univeristy, P.O.Box 2457, Riyadh 11451, Saudi Arabia, and* [3]*Department of Biochemistry, College of Science, King Saud Univeristy, P.O. Box 22452, Riyadh 11451, Saudi Arabia*

Молекулски докинг је обећавајућа и поуздана технологија за откривање наводећих једињења путем виртуелног скрининга. Поред тога што дозвољава тестирање великог броја једињења, он такође допушта одређивање како одабрана једињења инхибишу циљани протеин/рецептор на бази оцењивачке функције и рангирања. Пошто селективни инхибитори холинестеразе и моноамин оксидазе играју критичну улогу у третирању Алцхајмерове болести, ово истраживање се фокусира на расветљавање механизма везивних интеракција неколико хинолинских деривата у активним местима холинестеразе (ацетил-холинестеразе (AChE) и бутирилхолинестеразе (BChE) и моноамин оксидазе (MAO) (моноамин оксидазе A &B). Као резултат ових открића, могуће је да се новоидентификовани инхибитори употребе као наводећа једињења у развоју нових инхибитора ензима за третирање специфичних болести, па тако омогуће развој нових терапијских приступа.

(Примљено 7. марта; ревидирано 26. јуна; прихваћено 14. августа 2023.)

REFERENCES

1. J. M. Shine, E.J. Müller, B. Munn, J. Cabral, R. J. Moran, M. Breakspear, *Nat. Neurosci* **24** (2021) 765-776 (https://doi.org/10.1038/s41593-021-00824-6)
2. I. Gülçin, A. Scozzafava, C.T. Supuran, Z. Koksal, F. Turkan, S. Çetinkaya, S.H. Alwasel, *J. Enzyme Inhib. Med. Chem.* **31** (2016) 1698-1702 (https://doi.org/10.3109/14756366.2015.1135914)
3. J. Patočka, K. Kuča, D. Jun, *Acta med. (Hradec Kral.)* **47** (2004) 215-228 (https://actamedica.lfhk.cuni.cz/media/pdf/18059694.2018.95.pdf)
4. J. R. Atack, E. K. Perry, J. R. Bonham, J. M. Candy, R. H. Perry, *J. Neurochem.* **47** (1986) 263-277 (https://doi.org/10.1111/j.1471-4159.1986.tb02858.x)
5. B. Li, J. A. Stribley , A. Ticu, W. Xie, L. M. Schopfer, P. Hammond, O. J. Lockridge, *J. Neurochem.* **75** (2000) 1320-1331 (https://doi.org/10.1046/j.1471-4159.2000.751320.x_
6. C. N. Pope, S. Brimijoin, *Biochem. Pharmacol.* **153** (2018) 205-216 (https://doi.org/10.1016/j.bcp.2018.01.044
7. R. M. Geha, K. Chen, J. Wouters, F. Ooms, J. C. Shih, *J.Biol.Chem* **277** (2002) 17209-17216 (https://doi.org/10.1074/jbc.M110920200)
8. J. Grimsby, K. Chen, L. J. Wang, N. C. Lan, J. C. Shih, *Proceedings of the National Academy of Sciences* **88** (1991) 3637-3641 (https://doi.org/10.1073/pnas.88.9.3637)

9. R.M. Geha, I. Rebrin, K. Chen, J.C. Shih. Substrate and inhibitor specificities for human monoamine oxidase A and B are influenced by a single amino acid. *J. Biol. Chem.* **276** (2001) 9877-9882 (https://doi.org/10.1074/jbc.M006972200)

10. J. Grimsby, N. C. Lan, R. Neve, K. Chen, J. C. Shih, *J Neurochem.* **55** (1990) 1166-1169 (https://doi.org/10.1111/j.1471-4159.1990.tb03121.x)

11. K. N. Westlund, R. M. Denney, L. M. Kochersperger, R. M. Rose, C. W. Abell, *Science* **230** (1985) 181-183 (https://doi.org/10.1126/science.3875898)

12. R. J. Castellani, R. K. Rolston, M. A. Smith, *Disease-a-month* **56** (2010) 484 (https://dx.doi.org/10.1016%2Fj.disamonth.2010.06.001)

13. C. Geula, S. Darvesh, *Drugs of Today* **40** (2004) 711-721 (https://doi.org/10.1358/dot.2004.40.8.850473)

14. M. Mesulam, A. Guillozet, P. Shaw, B. Quinn, *Neurobiol. Dis*. **9** (2002) 88-93 (https://doi.org/10.1006/nbdi.2001.0462)

15. E. Giacobini, *Int. J. Geriatr. Psychiatry.* **18** (2003) S1-S5 (https://doi.org/10.1002/gps.935)

16. S. Darvesh, *Curr. Alzheimer Res.* **13** (2016) 1173-1177 (https://doi.org/10.2174/1567205013666160404120542)

17. Z. Cai, *Mol. Med. Rep.* **9** (2014) 1533-1541 (https://doi.org/10.3892/mmr.2014.2040)

18. S. Manzoor, N. Hoda, *Eur.J.Med.Chem*. **206** (2020) 112787 (https://doi.org/10.1016/j.ejmech.2020.112787)

19. P. O. Patil, S. B. Bari, S. D. Firke, P. K. Deshmukh, S. T. Donda, D.A. Patil, *Bioorg. Med. Chem.* **21** (2013) 2434-2450 (https://doi.org/10.1016/j.bmc.2013.02.017)

20. G. Nesi, S. Sestito, M. Digiacomo, S. Rapposelli, *Curr Top Med Chem.* **17** (2017) 3062-3079 (https://doi.org/10.2174/1568026617666170607114232)

21. L. Mucke, *Nature* **461** (2009) 895-897 (https://doi.org/10.1038/461895a)

22. L. Blaikie, P. Kay, P.K.T. Lin, *MedChemComm*, **10** (2019) 2052-2072 (https://doi.org/10.1039/C9MD00337A)

23. T. Tomašić, L. Peterlin Masic. *Curr. Top. Med. Chem.* **14** (2014) 130-51 (https://doi.org/10.2174/1568026613666131113153251)

24. J. H. Xu, Y. L. Fan, J. Zhou, *J. Heterocycl. Chem.* **55** (2018) 1854 (https://doi.org/10.1002/jhet.3234)

25. Chemical Computing Group, M. O. E. Molecular Operating Environment. Chemical Computing Group Montreal, Quebec, Canada.**2008**

26. BioSolveIT-SeeSAR. https://www.biosolveit.de/SeeSAR